S.C. Löhr, E.T. Baruch, P.A. Hall, M.J. Kennedy
Is organic pore development in gas shales influenced by the primary porosity and structure of thermally immature organic matter?
Organic Geochemistry, 2015; 87:119-132

Originally published at:
http://doi.org/10.1016/j.orggeochem.2015.07.010

Organic Geochemistry 87 (2015) 119–132

Contents lists available at ScienceDirect

Organic Geochemistry

journal homepage: www.elsevier.com/locate/orggeochem

Is organic pore development in gas shales influenced by the primary porosity and structure of thermally immature organic matter?

S.C. Löhr [a,*], E.T. Baruch [b,1], P.A. Hall [b], M.J. Kennedy [a]

[a] Department of Earth & Planetary Sciences, Macquarie University, North Ryde 2109, Australia
[b] Sprigg Geobiology Centre & Department of Earth Sciences, University of Adelaide, Adelaide, SA 5005, Australia

ARTICLE INFO

Article history:
Received 23 April 2015
Received in revised form 27 July 2015
Accepted 28 July 2015
Available online 5 August 2015

Keywords:
Organic-hosted porosity
Thermal maturation
Pore characterisation
Unconventional shale reservoir
SEM
Organic matter diagenesis
Kerogen
Bitumen
Pore network

ABSTRACT

Organic matter (OM)-hosted pores, rather than mineral-hosted pores, are considered to be the dominant contributors to total porosity and hydrocarbon storage in many organic-rich unconventional reservoirs. OM-hosted pores are thought to develop during thermal maturation as generated hydrocarbons are expelled from the kerogen, leaving behind pores. However, prediction of OM-hosted pore development is hampered by the lack of a simple relationship between thermal maturity and OM-hosted porosity, with the controls on pore distribution, size and morphology remaining poorly known. In particular, the extent to which thermally immature OM hosts primary pores and the influence that these have on subsequent organic pore development remains poorly understood. Here we employ Ar ion beam polishing and high resolution scanning electron microscopy to show that primary OM-hosted pores are common in thermally immature shales of varying ages and depositional settings, where they occur in both structured and amorphous OM. We further find, utilising a thermal maturity gradient in the Devonian-Mississippian Woodford Shale, that although OM-hosted pores are common in the least mature (< 0.4 %Ro) samples imaged they are not evident in examples that are mature (0.5–1.1 %Ro). However, OM-hosted pores similar to those observed in the least mature samples are present in gas-mature samples (⩾ 1.5 %Ro), where they are classified as secondary pores. Solvent extraction to remove bitumen from oil-mature samples results in an abundance of pores in samples where previously none were evident, which suggests that the absence of primary OM-hosted pores in untreated oil-mature samples is due to infilling of pores by generated and retained bitumen. The similar size and morphology of more complex secondary pores and primary pores is consistent with re-emergence of primary pores in gas-mature structured organic matter, following expulsion of infilling bitumen. Inheritance of pore structure is less evident in amorphous OM types, where secondary pores exhibit a distinctive spherical morphology that has previously been attributed to a gas bubble origin within bitumen. However, similar spherical pore morphologies are evident in immature amorphous OM, arguing against a maturation related origin, so that re-emergence of primary pores cannot be ruled out. Our findings are also relevant to models of hydrocarbon storage and migration. Given that bitumen filled organic pores are likely open in regards to hydrocarbon migration, the importance of organic pore networks for primary migration in the oil window may have been underestimated – well developed organic pore networks contributing to permeability and storage capacity are otherwise assumed to be a feature characteristic of gas-mature shale reservoirs.

1. Introduction

The study of mudrocks has long focused on their qualities as seals in conventional hydrocarbon systems or for their generative potential as source rocks. However, recent trends in shale oil and gas production have demonstrated that mudrocks can be (unconventional) hydrocarbon reservoirs in their own right. The capacity of fine grained sediments to act as economic reservoirs is largely dependent on their storage capacity, permeability and potential for fracture stimulation. The pores, along with natural fractures, form the flow path network that allows flow of oil or gas from the mudrock to induced fractures during production. Determining the type, quantity and arrangement of pores is thus of central

* Corresponding author.
E-mail address: stefan.loehr@mq.edu.au (S.C. Löhr).
[1] Current address: Origin Energy Ltd, 339 Coronation Drive, Milton, QLD 4064, Australia.

http://dx.doi.org/10.1016/j.orggeochem.2015.07.010
0146-6380/

importance to any assessment of shale reservoir quality (Loucks et al., 2012; Milliken et al., 2013). In addition, the ability to predict porosity trends along thermal maturation or burial gradients is an important component of successful well placement. Prediction of porosity trends requires, in turn, a fundamental understanding of mudrock pore types and the controls on their distribution and development.

Pore networks in mudrocks are composed of nanometre- to micrometre-size pores. Three broad pore classes are recognised (Loucks et al., 2012): (1) interparticle pores, (2) mineral-hosted intraparticle pores and, (3) intraparticle, organic matter (OM)-hosted pores. Here we refer to the latter as OM-hosted pores. Mudrock porosity and pore evolution have been studied mainly through direct high resolution imaging techniques such as scanning electron microscopy (SEM; Curtis et al., 2012a; Milliken et al., 2013) or, alternatively, bulk characterisation techniques such as gas adsorption, mercury intrusion, or small-angle neutron scattering (Mastalerz et al., 2013; Bahadur et al., 2015). An advantage of the bulk pore characterisation techniques is that they provide quantitative assessments of pore volumes and pore size distribution, including < 10 nm size pores that cannot readily be imaged. However, bulk characterisation techniques cannot distinguish OM-hosted pores from mineral-hosted intra or interparticle pores, this requires high resolution imaging.

OM-hosted pores are mainly of sub-μm size, and are widely recognised as a significant component of the pore system in proven gas shales including the Barnett Shale (Loucks et al., 2009), the Woodford and Horn River shales (Curtis et al., 2012a; Loucks et al., 2012) and the Marcellus Formation (Milliken et al., 2013). Three-dimensional reconstructions of kerogen and porosity distribution using focused ion beam milling – SEM show that OM-hosted pores have the potential to form connected pore networks in organic-rich shale gas reservoirs such as the Barnett, Woodford and Horn River shales (Curtis et al., 2012b), where between 26–67% of the pore volume is connected. Although pores are typically divided into several separate pore networks, and individual pore networks rarely span the entire length of an analysed rock volume (Curtis et al., 2012b), a potentially dominant contribution of organic porosity to total porosity is indicated by the positive correlation between bulk TOC and total porosity in moderately OC rich, gas-mature mudrocks such as the Marcellus Formation (Milliken et al., 2013). These observations have resulted in the prediction that a greater potential for gas storage and gas flow exists in higher TOC mudrock intervals, depending on the abundance and connectivity of the OM-hosted pores (Loucks et al., 2012). From an unconventional reservoir perspective, therefore, it comes as no surprise that there has been a sustained effort to determine the controls on size, abundance, distribution and morphology of OM-hosted pores (Fishman et al., 2012; Mastalerz et al., 2013; Milliken et al., 2013; Valenza et al., 2013). The controls on porosity evolution and distribution with diagenesis and OM maturation, however, remain poorly known.

The common working model of organic pore genesis holds that the abundance of organic hosted pores is largely a function of thermal maturity, so that porosity increases with thermal maturity (Loucks et al., 2012). According to this model, OM-hosted pores develop due to the thermal cracking of sedimentary OM (also termed kerogen), which generates hydrocarbons that are subsequently expelled from the kerogen structure, leaving behind pores. Alternatively, the commonly bubble-like pore morphology in gas-mature samples of the Marcellus and New Albany Shales have been interpreted as evidence that these pores form as gas bubbles within quasi-solid bitumen after secondary cracking of bitumen in the gas window (Milliken et al., 2013; Schieber, 2013). The link between organic pore abundance and thermal maturity is inferred from high resolution SEM-based studies of thermal maturity gradients within proven gas shales such as the Woodford (Curtis et al., 2012a) and Barnett Shale (Bernard et al., 2012). In these studies organic pores are rarely evident in samples from the early oil window, but are more commonly observed in samples from the late oil window (> 0.9 %Ro) and are generally most abundant in gas and overmature samples, collected from deeper parts of the basin in question. In addition to direct high resolution imaging evidence, bulk porosity measurements of 30 mudrock samples from several gas shale basins across North America showed greater pore volumes and smaller mean pore diameters in more thermally mature samples relative to less thermally mature ones (Valenza et al., 2013). The authors of that study interpreted this to reflect the development of nm-size organic pores in kerogen at greater thermal maturities, although this was not confirmed directly by high resolution imaging.

There remain, however, several important gaps in the understanding of organic pore development. Organic matter pores in the Jurassic Kimmeridge Clay were found to be largely similar in terms of size, shape and abundance (Fishman et al., 2012), regardless of maturity, although there were differences between OM types at a given maturity. The SEM study by Curtis et al. (2012a) of a Woodford Shale thermal maturity gradient (samples from 8 different wells, ranging between 0.5–6.4 %Ro), on the other hand, shows that OM-hosted pores are generally more abundant in gas-mature samples compared to oil-mature ones. However, they did not observe a linear relationship between OM-hosted porosity and thermal maturity, as might be expected if maturation was the only control on pore abundance. Instead, their study revealed marked small-scale heterogeneity in distribution of OM-hosted pores, both within single OM domains where pores can cluster or be equally spaced, and between adjacent OM grains where one grain might show an abundance of pores whereas the adjacent grain has none (Curtis et al., 2012a). Similarly heterogeneous pore distribution is evident in oil and gas-mature samples of the Marcellus Formation (Milliken et al., 2013) where, additionally, organic pore abundance and size varies as a function of OM abundance rather than thermal maturity. Oil-mature samples with > 5% TOC were shown to have reduced porosities and smaller mean pore diameters compared to lower TOC samples of identical thermal maturity and from the same sedimentary sequence (Milliken et al., 2013). Overall, these observations show that: (a) potential OM-hosted porosity is strongly influenced by OM type, and (b) OM-hosted porosity varies greatly within and between samples of a given thermal maturity, even where these are from the same lithofacies and the same formation. An important role for OM type in determining OM porosity pathways is consistent with the contrasting hydrocarbon generation potential of OM types such as gas-prone woody terrigenous vs oil-prone algal marine OM (Hunt, 1996). The structured pore distribution evident in some gas-mature organic particles (Loucks et al., 2012) further suggests that organic pore morphology and distribution is influenced by OM type.

Most work to date has utilised natural thermal maturity gradients, comparing samples from the same sedimentary sequence but subject to different burial depths and temperatures. Although the presence of pores in immature sedimentary organic material has long been recognised, the great majority of studies of organic pore development have not included samples from the thermally immature end of the spectrum, with the least mature samples included in these gradients generally of early to late oil maturity ($\geqslant$ 0.5 %Ro). Yet without systematically investigating thermally immature samples the extent to which the pore system is primary, i.e. hosted within initially porous kerogen, vs secondary (i.e. later formation) cannot be assessed. Furthermore, only in thermally immature OM can those primary OM features which have the potential to influence later pore development be identified (Milliken et al., 2014);

features which may explain the OM type dependency of OM-hosted porosity observed in previous studies (Fishman et al., 2012; Milliken et al., 2013). Thus, careful analysis of immature samples is required to assess the influence of primary porosity and inherited OM structure on subsequent pore placement, structure and development.

In this study we employed high resolution scanning electron microscopy to determine the abundance and nature of pores associated with organic matter in high TOC, thermally immature mudrocks of differing ages, OM types and depositional settings. We show that primary porosity within OM is a feature common to many thermally immature mudrocks. We subsequently apply this approach to assess OM porosity in samples of varying thermal maturity in the Devonian-Mississippian Woodford Shale, including thermally immature samples. Our results show that the porosity characteristic of thermally immature OM is not apparent in oil-mature intervals until after pore-filling bitumen has been removed by solvent extraction, but OM-hosted pores are again evident in samples from the gas window without requiring solvent extraction. We discuss to what extent the primary porosity and inherited OM structure influences secondary OM porosity, and the implications for interpreting the results of previous studies.

2. Materials and methods

2.1. Materials

We collected samples from four organic-rich, thermally immature mudrocks (Table 1), containing various classes of OM ranging from amorphous OM associated with the clay mineral matrix at μm to nm scales to large structured organic particles of marine and terrigenous origin. Some of these are immature samples of intervals with proven unconventional reservoir potential at higher thermal maturities, others are representative of classical low-oxygen or more unusual cold-climate source rocks which may have unconventional potential at greater burial depths. These include: (a) the Miocene Monterey Fm, a well know oil shale that is both source and reservoir for major quantities of hydrocarbons onshore and offshore California, (b) Cretaceous, hemipelagic black shales from Demerara Rise (equatorial North Atlantic), representative of the classic Oceanic Anoxic Event black shales that source a disproportionate percentage of globally producible hydrocarbons (Takashima et al., 2006), (c) the end-Permian Stuart Range Fm of South Australia, an unusual cold climate, pyrite and organic matter enriched mudrock which is a current source rock/unconventional reservoir target, and (d) the Devonian-Mississippian Woodford Shale, which is a proven unconventional shale gas reservoir in more thermally mature locales (Slatt et al., 2011). We also collected Woodford Shale samples ranging between 0.5–3.1 %Ro, representing a complete thermal maturity gradient through which to assess changes to OM porosity with thermal maturity.

The Monterey Formation (18.4–6.7 Ma) is a low-gradient slope, open margin deposit (Isaacs, 2001) with organic matter that is primarily of marine origin (Graham and Williams, 1985). Thermally immature samples were obtained from the middle phosphatic facies (066105-61) and the lower calcareous facies (022406-41) at the Naples Beach section of the Monterey Formation, located east of the Dos Pueblos Creek, 25 km west of Santa Barbara, within the Santa Barbara/Ventura Basin (Isaacs, 2001). This section is regarded as a classic type locality for the Monterey Formation, due to its low thermal maturity, excellent exposure and freshness of weathering. Mineralogy of the studied samples is comprised mainly of quartz, calcite, illite, mixed-layer illite/smectite, kaolinite, albite, apatite, pyrite and zeolite.

Cenomanian to Santonian black shale sequences, including the Oceanic Anoxic Event 2 interval, were recovered at Demerara Rise, in the western equatorial Atlantic Ocean, during Ocean Drilling Program (ODP) Leg 207 (Shipboard Scientific Party, 2004). These represent lateral, immature equivalents of important source intervals in Venezuela and Colombia (e.g. La Luna Fm) (Bralower and Lorente, 2003), and comprise hemipelagic deposits with decimeter- to meter-scale cyclic alternations between carbonate-rich and organic-rich sediments (Nederbragt et al., 2007). A strong link between smectite clay abundance and enrichment of the dominantly marine OM has been identified, suggesting a clay mineral preservative effect on OM in this classic greenhouse anoxic facies (Löhr and Kennedy, 2014). Powder X-ray diffraction shows that the studied samples are comprised mainly of calcite, smectite, illite, quartz, biogenic opal, zeolite, apatite and pyrite.

The Stuart Range Formation (Permo-Carboniferious Arckaringa Basin, central-northern South Australia) is an organic-rich mudrock comprising chemically immature, coarse silt mineralogy associated with the end-Permian deglaciation (Menpes, 2012) and abundant (up to 30 wt%) framboidal pyrite. The Stuart Range Formation is dominated by massive and laminated black mudstone facies featuring abundant, well-preserved terrigenous (sporinite) and marine (alginate, lamalginite) liptinite incorporating high concentrations of sulfur, as well as lesser quantities of vitrinite and inertinite. Mineralogy of the studied samples comprises mainly quartz, pyrite, Na and K-feldspars, mica, illite, kaolinite and smectite.

The Devonian-Mississippian Woodford Shale is an economically important unconventional shale gas reservoir in the United States. It is an organic-rich marine mudstone preserved within a series of basins in modern day Texas, Oklahoma and southeastern New Mexico. OC enrichment has been attributed to the combined effects of slow sedimentation, anoxic preservation (Kirkland et al., 1992; Miceli Romero and Philp, 2012) and the stabilization of OC by clay mineral surfaces (Kennedy et al., 2014). The OM is mostly of marine origin (Comer, 1991), with a minor contribution of terrigenous, woody material. We collected samples representing a complete thermal maturity gradient, with calculated thermal maturities ranging between 0.34–3.10 %Ro, from several cores intersecting the Woodford Shale. Core names, locations, sampling depth and bulk sample properties including thermal maturity and TOC are listed in Table 1. Powder X-ray diffraction of samples from the Chitwood-Harris core (ca. 1 %Ro) shows that mineralogy of the Woodford Shale is comprised mainly of quartz, illite, pyrite, apatite, as well as K-feldspars, chlorite and dolomite in the less mature (%Ro < 0.4), less diagenetically altered East Fitts samples.

2.2. Bulk sample characterisation

Total carbon (TC) content for each sample was measured in a Perkin Elmer 2400 Series II CHNS analyser. Inorganic carbon (IC) content was determined using the pressure-calcimeter method of Sherrod et al. (2002). OC content was calculated by difference (TOC = TC − IC).

Thermal maturity and hydrocarbon generation potential of each sample was determined by pyrolysis using a Weatherford Instruments Source Rock Analyser. Thermal maturity was estimated using the method of Jarvie et al. (2001), which relates measured T_{max} to calculated vitrinite reflectance using the following relationship: calculated %Ro = 0.0180 × T_{max} − 7.16. Calculated thermal maturities > 1.1 %Ro were verified by comparison with vitrinite reflectance values (courtesy of Brian Cardott, Oklahoma Geological Survey).

2.3. SEM imaging and analysis

OM distribution, morphology and porosity were imaged using a FEI Quanta 450 high resolution, field emission environmental

Table 1
Sample details.

Age	Formation	Location	Core or Site	Sample ID or depth (ft/m)	Calc. % Ro	Kerogen Type	TOC (%)	HI	S1	S2
Early Permian	Stuart Range	Arckaringa Basin South Australia	Arck1 core, Boorthana Through	L1	0.46	II	5.8	279	0.31	16.2
Early Permian	Stuart Range	Arckaringa Basin South Australia	Arck1 core, Boorthana Through	2053196 (3149.5 ft/ 959.97 m)	0.48	II	7.7	330	0.7	25.5
Cenomanian/ Turonian	"OAE 2 black shale"	Demerara Rise Equatorial North Atlantic	ODP Site 1258	1258/43/3 60-61 cm	< 0.35	II	10.4	569	1.12	59.2
Cenomanian/ Turonian	"OAE 2 black shale"	Demerara Rise Equatorial North Atlantic	ODP Site 1258	1258/43/3 70-71 cm	< 0.35	II	12.0	639	1.66	76.6
Miocene	Monterey	California, USA	Naples Beach	022406 41	< 0.35	II S	9.6	706	1.42	67.4
Miocene	Monterey	California, USA	Naples Beach	066105 61	< 0.35	II S	18.8	414	1.75	77.8
Devonian	Woodford	Pontotoc County, Oklahoma	Wyche #1 core	WEB 94 (153.7 ft/ 46.86 m)	< 0.35	II	8.2	519	1.83	42.8
Devonian	Woodford	Pontotoc County, Oklahoma	Wyche #1 core	WEB 71 (131.1 ft/ 39.97 m)	0.44	II	12.9	495	2.03	63.8
Devonian	Woodford	Pontotoc County, Oklahoma	Wyche #1 core	WEB 65 (124.8 ft/ 38.05 m)	0.38	II	11.1	472	1.56	52.6
Devonian	Woodford	Pontotoc County, Oklahoma	East Fitts core	3412 ft/1040 m	0.51	II	10.1	509	2.89	51.1
Devonian	Woodford	Pontotoc County, Oklahoma	East Fitts core	3420.1 ft/1042.4 m	0.51	II	15.8	473	4.53	74.6
Devonian	Woodford	Lincoln County, Oklahoma	Pritchard core	5132.7 ft/1564.4 m	0.66	II	8.9	509	4.02	45.4
Devonian	Woodford	Lincoln County, Oklahoma	Pritchard core	5150 ft/1569.7 m	0.67	II	8.6	479	4.18	41.3
Devonian	Woodford	Grady County, Oklahoma	Chitwood-Harris core	14911.9 ft/4545.1 m	0.95	II	5.2	22	0.79	1.15
Devonian	Woodford	Grady County, Oklahoma	Chitwood-Harris core	14935 ft/4552.2 m	1.00	II	10.3	30	1.54	3.12
Devonian	Woodford	Okfuskee County, Oklahoma	Holt core	3690.8 ft/1125 m	1.09	II	2.9	91	1.48	2.61
Devonian	Woodford	Okfuskee County, Oklahoma	Holt core	3708.9 ft/1130.5 m	0.96	II	8.5	93	2.21	7.90
Devonian	Woodford	Grady County, Oklahoma	Richardson core	13221 ft/4029.8 m	1.51 (1.46*)	II	6.2	35	0.79	2.17
Devonian	Woodford	Grady County, Oklahoma	Richardson core	13211 ft/4026.7 m	1.52 (1.46*)	II	5.9	30	0.56	1.79
Devonian	Woodford	Hemphill County, Texas	Mathers Ranch	McM#5	3.10*	II	8.5	ND	ND	ND

* Denotes vitrinite %VRo of Woodford Fm in the core (courtesy of Brian Cardott, Oklahoma Geological Survey).

scanning electron microscope (SEM) equipped with a backscattered electron (BSE) detector and energy dispersive X-ray (EDX) analyser. Prior to imaging samples were fixed onto SEM stubs with the imaged surface prepared perpendicular to bedding. Samples were oven-dried for 48 h at 60 °C and gently ground on corundum abrasive paper until flat. After cleaning with compressed nitrogen, the samples were ion milled until polished (Fischione 1060 Ar Ion Mill system) and coated with 5 nm Pt, or imaged in low vacuum mode without coating.

Exposure to vacuum during sample preparation and imaging can result in desiccation features, including the formation of pores in organic macerals (Fishman et al., 2012; Schieber, 2013). However, pores induced by desiccation shrinkage or excessive exposure to the electron beam typically have a characteristic elongate, crack-like morphology and commonly occur at the interface between organic and inorganic domains. We use these criteria to distinguish them from naturally occurring pores, which are of varying morphologies and sizes, often complex, and typically occur within organic domains rather than at the boundaries to inorganic domains.

After the initial SEM imaging, a subset of ion-milled, uncoated samples were solvent extracted to assess whether primary organic pores are clogged by bitumen. To this end each sample was Soxhlet extracted for 72 h using a solvent mixture comprised of 93% dichloromethane and 7% methanol. The samples were subsequently air-dried before reimaging by SEM. This approach was taken here because primary OM (kerogen) cannot be readily distinguished from bitumen, a secondary phase that is the product of organic diagenesis, using only SEM-based petrographic criteria (Milliken et al., 2014). Kerogen is formally defined as organic material that is insoluble in alkaline solvents and common organic solvents, whereas bitumen is soluble in these (Hunt, 1996). A solvent extraction step to remove the bitumen, followed by re-imaging of the samples, can therefore help identify bitumen. However, this approach is complicated by the fact that insoluble forms of bitumen known as "solid bitumen" or "pyrobitumen" can also occur, particularly in overmature samples. See Milliken et al. (2014) for a detailed discussion of this topic.

Where required, BSE and SE images were subsequently processed in FIJI image editing software to improve contrast between OM and OM-hosted pores. FIJI was also used to measure pore sizes.

2.4. Organic petrology

Uncoated, ion-polished samples prepared for SEM analysis were also utilised for organic petrology. The optical characteristics of various macerals present within the samples were examined with a Nikon Ci Pol microscope using 5× to 100× air immersion objectives, under both reflected and UV fluorescent light. Maceral recognition and differentiation is primarily based on the morphology,

reflectance, internal texture, relief, inter-grain relationship and other optical properties of macerals, and followed standard organic petrology methods (Taylor et al., 1998; Suárez-Ruiz et al., 2012).

3. Results

3.1. Primary pores in thermally immature OM

3.1.1. Monterey Formation

The Monterey Formation samples imaged are dominated by brightly fluorescing (UV light) amorphous OM. Rather than being concentrated in discrete OM domains or recognisable organic detritus, the great majority of the OM is disseminated through the sediment (Fig. 1A), where it is closely associated with and aggregated with clay minerals (Fig. 1C), although there are also organic domains which contain little clay (Fig. 1B). The porous nature of the organo-clay matrix is notable, comprising a complex network of pores in the 200–500 nm size range (arrows), together with abundant pores < 80 nm (Fig. 1C). The pores tend to concentrate in clusters and are not uniformly distributed. The abundance of pores of similar size and structure both within the organo-mineral matrix and in OM domains containing almost no clays (Fig. 1B vs 1C) shows that the OM is inherently porous, and that the observed pore structure in not a product of clay-organic association. Although OM-hosted pores are mainly empty, they are commonly partially filled with authigenic carbonate micrite (Fig. 1D).

3.1.2. Demerara Rise black shales

Similar to the Monterey Formation, OM in Demerara Rise samples is dominantly amorphous, of marine origin (Meyers et al., 2006) and disseminated through the sediment, where it is closely associated with clay minerals (Fig. 2A and B; see also Löhr and Kennedy, 2014). Although nm-scale pores are present in the organo-clay matrix, it is not characterised by the pervasive porosity evident in the otherwise similar organo-mineral matrix of the Monterey Fm. On the other hand, rarer discrete OM domains contain few embedded clays, and are characterised by abundant equant, circular to angular pores, falling into two main size ranges (300–100 nm and < 50 nm; Fig 2C and D). These pores are present in the majority of discrete OM domains imaged but, as in the Monterey Fm samples, the pores are clustered rather than uniformly distributed within the OM domains.

3.1.3. Stuart Range Formation

Samples of the Stuart Range Formation contain a larger range of porous and non-porous OM, reflecting a mixed terrigenous and marine origin. The OM is interpreted to be of a terrigenous, higher plant origin (vitrinite and inertinite) based on high white light reflectance, lack of fluorescence under UV light and the distinctive curved, sharp edged appearance in light and electron micrographs appears non-porous in the SEM images (Fig. 3C). Note, however, that vitrinite typically contains abundant pores < 2 nm that cannot be imaged using SEM (Mastalerz et al., 2012). The Stuart Range Fm also contains abundant large OM particles interpreted as terrigenous spores (sporinite) based on their compressed oval shape, hollow centre and strong yellow fluorescence. SEM imaging shows that the organic matter comprising the spore wall is non-porous, however the central spore cavity is commonly only partially closed by compaction or diagenetic cementation, and can contribute to primary porosity. Laminae of discrete OM, interpreted as lamalginite due to their morphology and strong fluorescence under UV

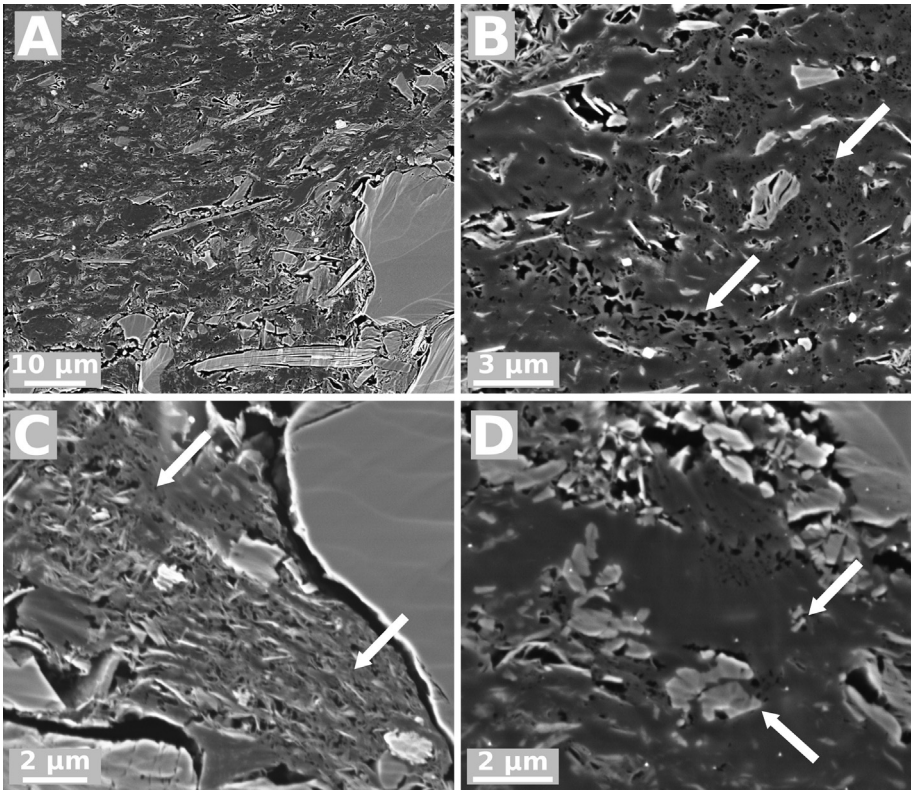

Fig. 1. (A) Monterey 022406-41, < 0.35 %Ro. Low-magnification image showing abundance of amorphous OM intimately associated with clay minerals and carbonate and quartz silt. (B) Monterey 022406-41, < 0.35 %Ro. Abundant pores in otherwise amorphous OM, with embedded clays. Pores are not homogeneously distributed through the OM, and are of variable size (compare smaller pores at top with larger pores at bottom). (C) Monterey 022406-41, < 0.35 %Ro: The bulk of OM is disseminated through the sediment, where it is associated with and aggregated with clay minerals. The porous nature of both OM-clay mixtures and the rarer relatively clay-free organic domains is notable, comprising a complex network of larger pores (200–500 nm size) as well as abundant pores < 80 nm (white arrows). (D) Monterey 066105-61, < 0.35 %Ro: Clay particles embedded in porous but otherwise amorphous OM domain. Arrows mark carbonate micrite, likely of microbial origin, filling some OM-hosted pores.

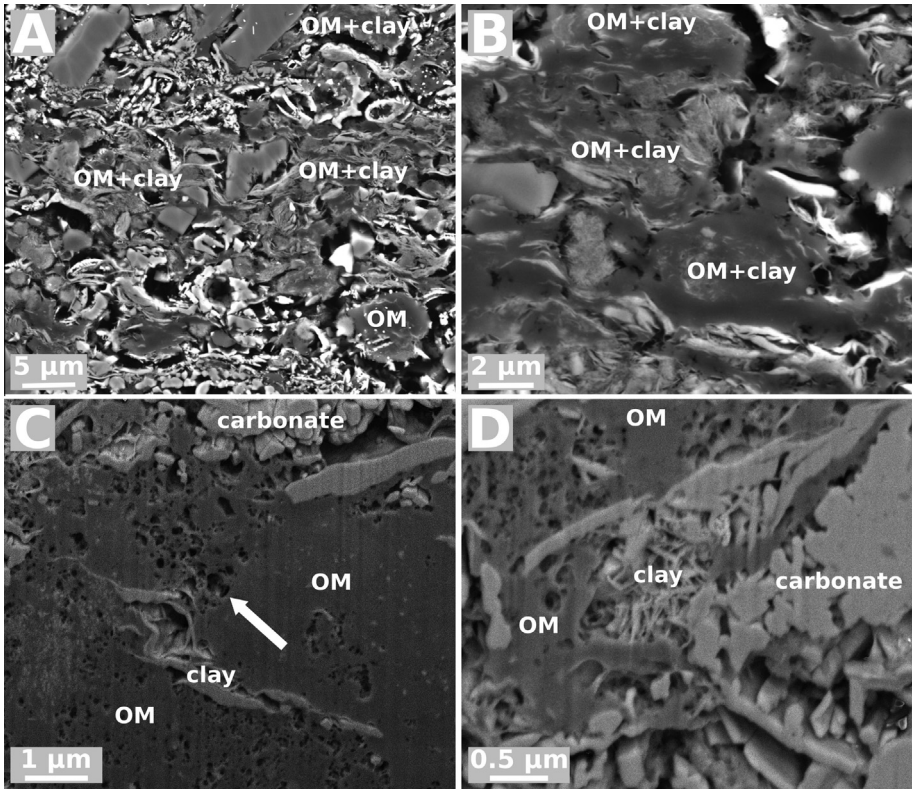

Fig. 2. (A) and (B) Demerara Rise, 1258/A/43R/3/60-61, < 0.35 %Ro: Amorphous OM is mainly present as organo-clay nanocomposites and aggregates, and is mostly non-porous. (C) Demerara Rise, 1258/A/43R/3/71-72, < 0.35 %Ro: Abundant, heterogeneously distributed organic pores in amorphous OM, with few embedded clays. (D) Demerara Rise, 1258/A/43R/3/71-72, < 0.35 %Ro. Abundant, heterogeneously distributed organic pores in amorphous OM, with few embedded clays.

light (Suárez-Ruiz et al., 2012), and hence likely of marine origin, are also generally non-porous. However, strongly fluorescing (under UV light) larger OM domains interpreted to be of colonial algal origin typically contain pores located between adjacent cells and within the membrane of individual cells, the result of only partial compaction and collapse of the individual cells comprising the algal colony (Fig. 3A). A subset of these pores is infilled by secondary cements such as quartz and apatite. Depending on compaction and cement infill, these pores may have a linear or wavy appearance in cross-section. In addition, larger (up to 30–40 µm size) domains of OM with irregular, uneven outline are commonly characterised by abundant porosity (Fig. 3B). These pore networks are dominated by two pore size classes: larger pores in the 1–2 µm size range and, substantially more abundant, pores in the 200–50 nm size range. Pores are mainly open and unfilled, but can be partially or entirely filled with apatite cement. Finally, aggregates of oblate, < 1 µm size OM domains are characterised by pores between individual OM domains, these are partially infilled by apatite (Fig. 3D).

3.2. The Woodford Shale thermal maturity gradient

Immature and early oil-mature Woodford samples (Wyche, East Fitts and Pritchard cores) contain abundant bright-yellow fluorescing liptinite particles, primarily thick walled Tasmanites (the phycoma of prasinophyte algae; Telnova, 2012), thinner-walled spores and colonial algae (Fig. 4A–C). Tasmanites and spores are concentrated in discrete intervals, so that their abundance varies substantially between, and even within, samples. In addition to these structured organic particles, which range between 30–280 µm in length, higher magnification reveals an abundance of weakly fluorescing < 5 µm amorphous OM (liptodetrinite) as well as lamalginite stringers, forming an organic network that is intimately associated with the fine grained matrix and difficult to distinguish in reflected white light. Non-fluorescent, high reflectance organic particles interpreted as woody debris (vitrinite and inertinite) are present at low abundances in samples of all thermal maturities. Palynological analysis of Woodford kerogen extracts (Senftle, 1989) shows that it is the amorphous, OM present within organo-mineral aggregates that represents the dominant contributor to TOC, rather than the visually more striking fluorescent and non-fluorescent structured organic particles, as also suggested by recent findings of a first order relationship between clay minerals and OM in the Woodford Shale (Kennedy et al., 2014).

While largely unchanged at lower thermal maturities, samples with > 0.9 %Ro show a different assemblage of OM macerals. OM is non-fluorescent, and large structured OM particles such as Tasmanites and colonial algae are comparatively rare. The absence of fluorescence can be attributed to the alteration of these most hydrogen-rich of macerals during thermal maturation (Suárez-Ruiz et al., 2012), whereas the low abundance of non-fluorescent Tasmanites remnants may equally be a reflection of the heterogeneous distribution of Tasmanites observed in less thermally mature samples. However, a network of < 5 µm amorphous OM associated with the mineral matrix remains, although now non-fluorescent. In addition, gas-mature samples show evidence of pore and fracture filling bitumen (Fig. 4). There is thus a different assemblage of both structured and amorphous OM in immature vs more mature samples.

BSE-SEM imaging of thermally immature, OC-rich samples of the Woodford Shale (Wyche core) identifies both porous and non-porous OM classes (Fig. 5A–D). While the large, discrete OM particles identified as woody detritus and Tasmanites appear non-porous in SEM images (Fig. 5C), three types of OM hosting

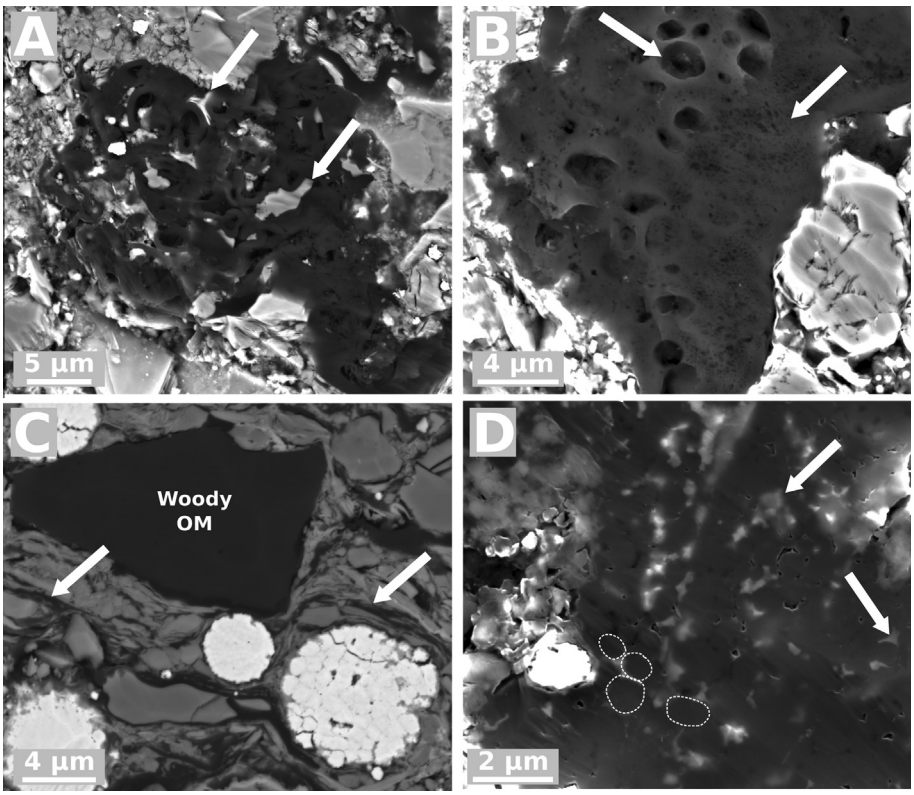

Fig. 3. (A) Stuart Ranges Fm L1, calc. 0.5 %Ro. OM of colonial algal origin typically contains both intracellular and intercellular pores due to partial collapse of the individual cells after compaction. Both intercellular and intracellular pores are commonly partially filled by secondary cements such as quartz or apatite (arrows). (B) Stuart Ranges Fm L1, calc. 0.5 %Ro. Large organic particle of unknown origin. Note the irregular outline and pervasive pore network dominated by two pore size classes: larger pores in the 1–2 µm size range and, substantially more abundant, pores in the 200 to 50 nm size range. Although open in this example, pores in similar OM particles are commonly filled with apatite cement. (C) Stuart Ranges Fm, ARC1, 2053196, calc. 0.48 %Ro. Woody OM of terrigenous origin appears non-porous in SEM images, as do the discrete OM laminae or stringers, interpreted as lamalginite. (D) Stuart Ranges Fm L1, calc. 0.5 %Ro. Aggregate of individual < 1 µm size, spherical to ovoid OM bodies (examples outlined) with pores between adjacent OM bodies. Most of these pores are infilled by apatite cement (brighter material shown by arrows).

visible pores where identified in these samples. (1) Porous amorphous OM (shown in Fig. 5A–D), mainly present as < 2 µm domains of OM encapsulated and separated by clay minerals and larger detrital grains, contains roughly equant pores. Larger pores are typically 200–100 nm, but pores as small as 30 nm diameter are present. Elongate OM stringers (interpreted as lamalginite) are similar, but host less abundant pores compared to smaller, equant OM domains which are encapsulated by clays and silt grains. Pores in amorphous OM represent the majority of organic pores in the Woodford Shale, with most thermally immature amorphous OM domains containing pores. However, pore abundance and size is highly variable, even between adjacent amorphous OM domains, potentially due to varying compaction (e.g. Schieber, 2013) or perhaps depositional or diagenetic differences. (2) Structured, colonial algal material with porosity retained within partially collapsed individual algal cells and between individual cells (Fig. 5A), as also observed in Stuart Range Fm samples. These pores are larger and more elongate than those observed within the 'amorphous' OM, at times resembling the elongate/slit-like pores observed in gas-mature structured OM by Loucks et al. (2012). (3) Pores between individual 900 and 400 nm diameter OM bodies that are concentrated into larger aggregates (Fig. 5A), similar to the Stuart Range Formation (see Fig. 3D). These pores are mainly 200–600 nm.

As in the immature Wyche samples, the majority of OM in the East Fitts and Pritchard core samples is present as amorphous OM domains packaged between and separated by detrital clay particles, or in lamalginite stringers, with structured particles such Tasmanites only of secondary importance. However, SEM imaging shows that none of the organic matter types in these samples of early oil window maturity (0.5–0.7 %Ro) contain pores (Fig. 6), apart from slit-like pores at organic-mineral grain boundaries that likely reflect artefacts of sample preparation or desiccation (Fishman et al., 2012). OM that was clearly of colonial algal origin or aggregates of < 1 µm, oblate OM domains were not observed in these samples.

Samples from the Chitwood Harris and Holt cores share similar thermal maturities between 0.95–1.09 %Ro. OM in these samples is present mainly in < 2 µm packets, encapsulated by clays and deformed by further compaction and growth of authigenic quartz, as well as stringers of more continuous OM (Fig. 7). Infrequent larger discrete OM particles are interpreted as woody, terrigenous OM or altered remnants of Tasmanites, consistent with UV microscopy results. OM-hosted porosity is largely absent in these samples, apart from rare slit-like pores interpreted as desiccation features.

Gas-mature Richardson core samples (1.52 %Ro), however, are characterised by several types of OM-hosted porosity (Fig. 8A–C). While pores are largely absent in large (> 10 µm) discrete OM domains, the more common smaller OM domains typically show an abundance of equant pores (Fig. 8B and C). These pores are somewhat more rounded than those in the immature Woodford OM, but the size range of the larger pores (80 and 140 nm) is similar to that of pores within immature amorphous OM. The nonporous, elongate OM domains may be altered Tasmanites, spores or lamalginite, OM classes that are present in the less thermally mature samples, but could equally be generated phases such as bitumen or pyrobitumen (Loucks and Reed, 2014). Unlike the oil-mature samples imaged, the gas-mature Richardson samples also

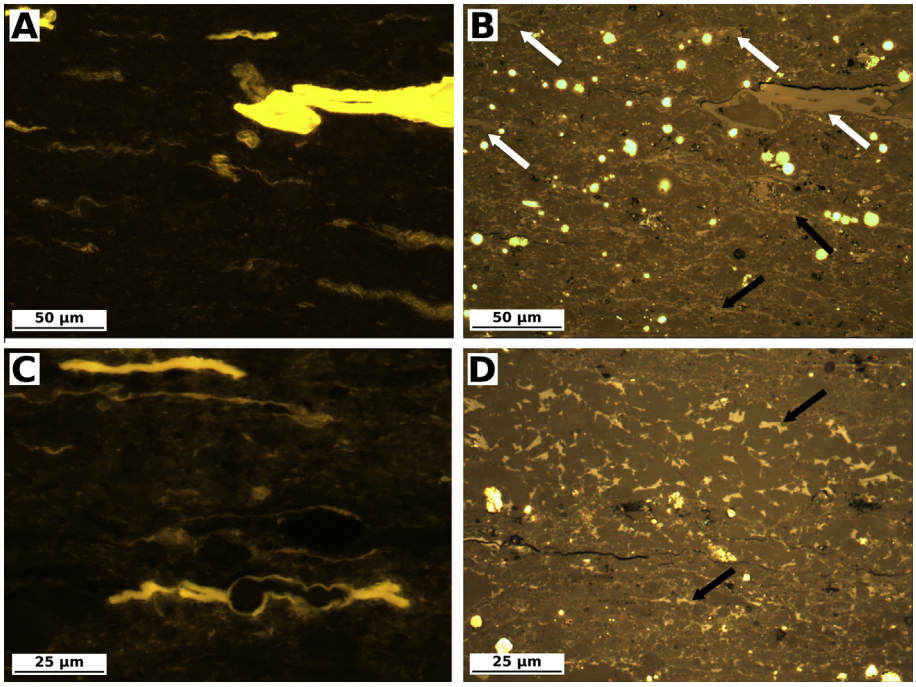

Fig. 4. Reflected white light and fluorescence mode photomicrographs of Woodford Shale samples of varying thermal maturity. (A) Fluorescence mode and (B) reflected white light, Pritchard 5132.7 (calc. 0.66 %Ro). Brightly fluorescing alginite (Tasmanites) and lamalginite are evident (white arrows), also dully fluorescing amorphous OM which imparts matrix fluorescence. Amorphous OM appears as a dense network of brighter material (black arrows) under reflected white light. (C) Fluorescence mode, Wyche 124.8 (calc. 0.38 %Ro). Large particles of yellow-fluorescing alginite, mainly Tasmanites, and lamalginite are prominent in Wyche samples. Matrix fluorescence is due to dully fluorescing amorphous OM that is closely associated with the mineral matrix. (D) Reflected white light, Chitwood Harris 14911.9 (calc. 0.95 %Ro). Large OM particles are mostly absent at higher thermal maturities, but a dense network of non-fluorescent amorphous OM persists (black arrows), although this may also be bitumen or pyrobitumen. (For interpretation of the references to colour in this figure legend, the reader is referred to the web version of this article.)

contain porous aggregates of the oblate, < 1 µm OM domains otherwise only observed in thermally immature samples.

OM-hosted pores in the overmature Mathers Ranch sample (3.1 %Ro) have a wide size distribution, ranging from 100s of nm in size to > 3 µm diameter, substantially larger than the typically 80–140 nm size pores within the gas-mature and thermally immature OM. The pores typically have irregular shapes that are very different to the round bubble-like pores typical of the Richardson core, and the shape of the larger pores is often defined by adjacent mineral grains confining the organic domain in which the pore has developed (Fig. 8D). However, as in lower thermal maturity samples, not all OM is porous. Adjacent OM domains of otherwise comparable morphologies may be non-porous, feature mainly nm-scale pores, or host µm-scale pores.

4. Discussion

Organic petrography and SEM analysis of immature, OC-rich mudrocks reveals various OM classes, ranging from structured organic detritus with a clear precursor (woody debris, prasinophyte algae, colonial algae) as well as various type of amorphous OM, including discrete amorphous OM in stringers or laminae, small organic domains encapsulated by clay minerals or organo-clay aggregates and composites. Structured OM types, in general, have consistent or predictable porosity styles. Woody material and Tasmanites do not contain pores sufficiently large to image by SEM, whereas partially compressed and cemented spores, colonial algae and aggregates of oblate OM domains are each associated with characteristic pore styles. Amorphous OM types, on the other hand, are more variable. Mixed organo-clay domains feature pervasive, abundant porosity in the Monterey Fm (Fig. 1) samples imaged here, whereas the organo-clay aggregates of the Demerara Rise black shale are largely devoid of pores. In the Demerara Rise samples it is the rarer, discrete amorphous OM domains which are characterised by pervasive, if unevenly distributed, porosity (Fig. 2). Similarly, the bulk of OM porosity in the Woodford Shale is present within OM domains encapsulated by clays (Fig. 5). Although also comprising amorphous OM, discrete OM laminae or lamalginite host a moderate number of pores in the Woodford Shale but not in the Stuart Range Fm. The distribution and abundance of pores within individual amorphous OM types is also more varied when compared to the structured OM classes, so that the abundance of OM-pores can differ greatly even between adjacent, immature, amorphous OM domains. These differences may reflect differential compaction (Milliken et al., 2014; Schieber, 2013) or inherent variability in OM structure at deposition.

It is likely that the distribution of OM within mudrocks also plays a role in the preservation of primary OM-hosted pores. Milliken et al. (2014) recently used SEM petrography techniques to examine thermally immature, marine OM in Pliocene sapropels from the Eastern Mediterranean Basin, aiming to obtain analogue data for the assessment of organic-hosted pore development in oil and gas shales. Comparison of their results to our study shows some important differences, most notably the concentration of sapropel OM in discrete, bedding-parallel laminae, deformation of OM due to compaction, and almost entire absence of pores in the dominantly amorphous OM. Although some large organic particles such as algal spores host intergranular pores, this is rare. A dominance of non-porous, amorphous OM concentrated in discrete laminae is also confirmed by our recent study of sapropel microfabric (Löhr and Kennedy, 2015). On the basis of these results we suggest that where OM is concentrated in discrete, laterally continuous sheets (laminae in cross-section), it is particularly prone to compaction, bringing with it ductile deformation of OM, loss of any OM-hosted pores, and even filling of intergranular mineral-hosted pores by deformed OM (Milliken et al., 2014). OM-hosted

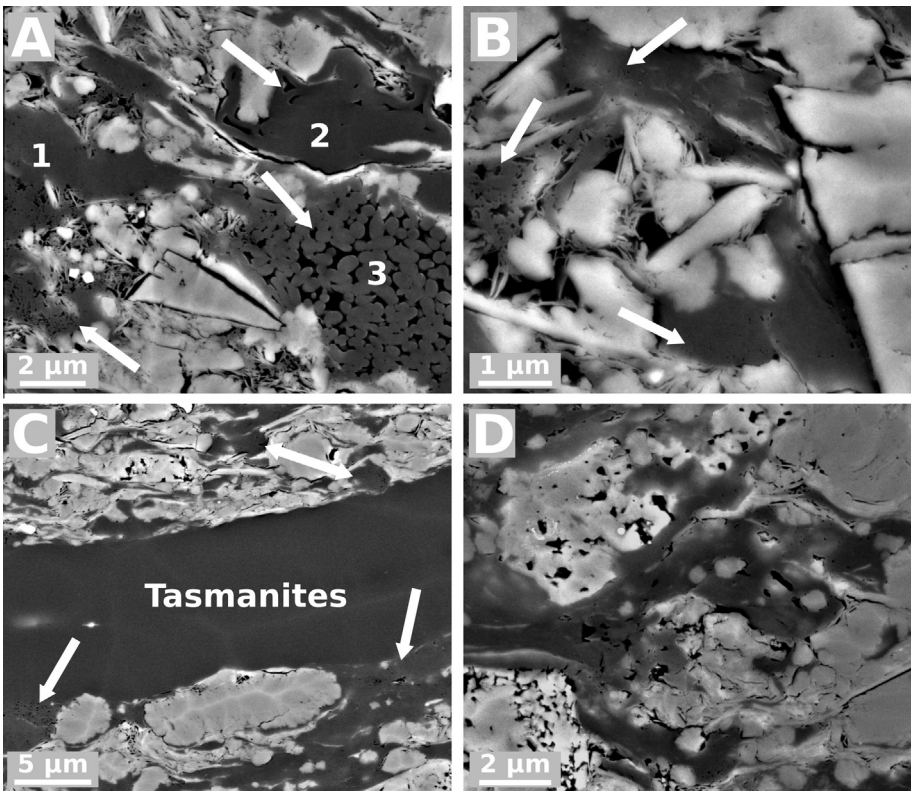

Fig. 5. SEM micrographs of immature Woodford Shale samples. (A) Wyche 153.7, calc. 0.38 %Ro. Three types of porous OM are recognised in the immature Woodford shale (marked from 1 to 3 on image). (1) Porous 'amorphous' OM, with a honeycomb-like or alveolar pore structure. Larger pores are typically 200–100 nm, but pores as small as 30 nm diameter are present. Pores are roughly equant. (2) Structured, colonial algal material with porosity retained within partially collapsed individual algal cells and between individual cells. These pores are larger and more elongate than those in the 'amorphous' OM. (3) Porosity between 900–400 nm diameter spherical OM bodies, concentrated within a 7 µm aggregate. These pores are also large, 200–600 nm. Type 1 represents the majority of OM in the Woodford shale, but types 2 and 3 are common. (B) Wyche 153.7, calc. 0.38 %Ro. Porous amorphous OM domains separated and encapsulated by clay and diagenetic cements. While the OM domain on the left hosts the largest, most obvious pores, all OM domains pictured contain pores. (C) Wyche 131.1, calc. 0.44 %Ro. In addition to porous, amorphous OM, large Tasmanites are common in the Woodford Shale; these invariably appear non-porous on SEM images. Note the sharp boundary between porous, amorphous OM and non-porous Tasmanites. (D) Wyche 131.1, calc. 0.44 %Ro. Amorphous, porous OM adjacent to porous carbonate grain.

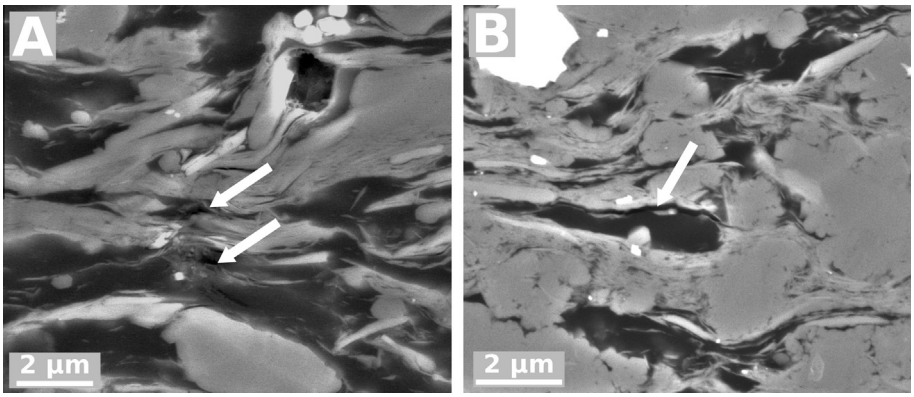

Fig. 6. SEM micrographs of Woodford Shale samples of early oil window maturity. (A) East Fitts 3412, calc. 0.51 %Ro. Typical example of amorphous OM domains separated and encapsulated by clays, mica and diagenetic quartz. No pores apparent within the OM, pores at this thermal maturity are restricted to intra- and interparticles pores in the mineral matrix. (B) Pritchard 5132.7, calc. 0.66 %Ro. Amorphous OM is non-porous apart from slit-like pores at OM-mineral interfaces (arrows), these are potential desiccation artifacts.

pores are more likely to be preserved where compaction of small OM domains is hindered by the presence of sheltering rigid framework grains (Schieber, 2013). The preservation of OM-hosted pores in the majority of immature mudrocks studied here vs the almost complete lack of primary OM-hosted pores in the amorphous marine OM of the sapropels and the Stuart Range Fm (Fig. 3C) may thus be a product of varying compaction, controlled by differing OM distribution within the mudrock, rather than differences in initial pore abundance.

While not all classes of immature OM are porous, and pore abundance is markedly variable even in OM of the same type within a single sample, the presence of OM-hosted pores in thermally immature samples suggest that these pores are primary features characteristic of particular classes of sedimentary OM. Pores

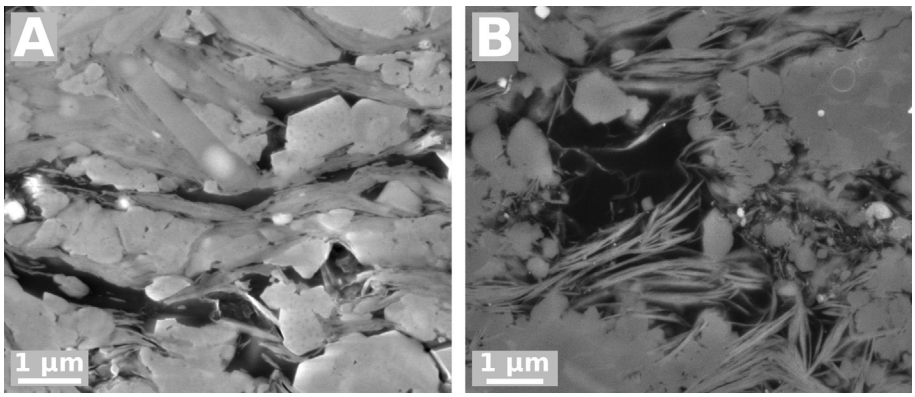

Fig. 7. SEM micrographs of Woodford Shale samples of late oil window maturity. (A) Chitwood Harris 14911.9, calc. 0.95 %Ro. Amorphous OM is non-porous. (B) Holt 3690.8, calc. 1.09 %Ro. Non-porous, amorphous OM encapsulated by clays and quartz cements.

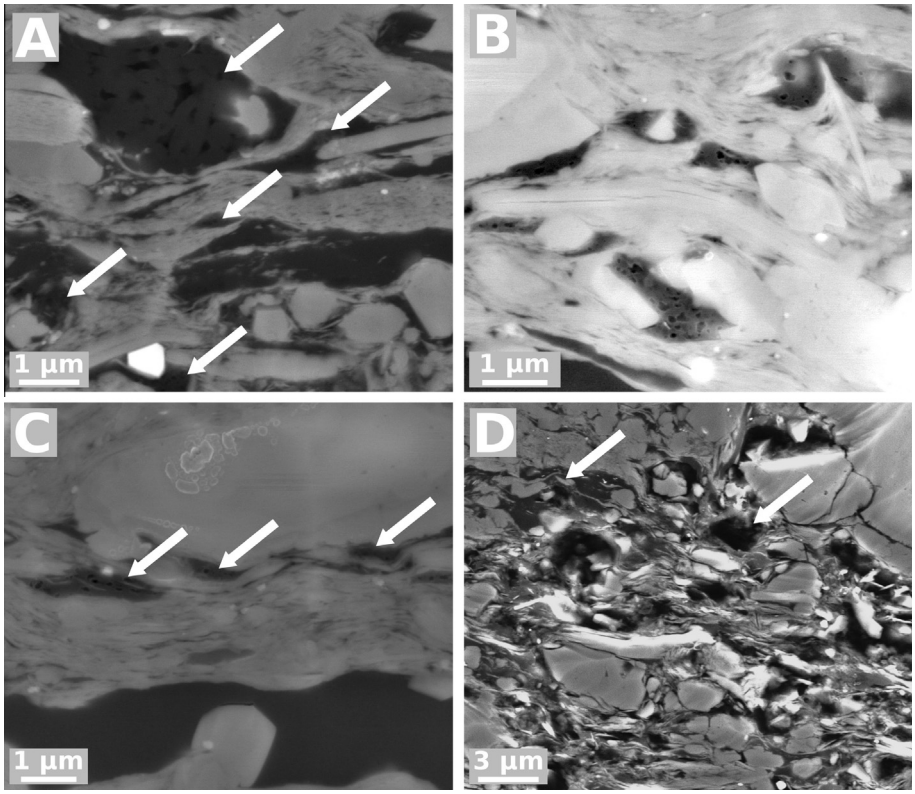

Fig. 8. SEM micrographs of gas-mature and overmature Woodford Shale samples. (A) Richardson 13221, calc. 1.51 %Ro. Pores in aggregate of ovoid OM bodies (top left). Similar aggregates were also observed in immature Woodford (Fig. 5A) and Stuart Range Fm samples (Fig. 3D). Pores are also evident within the smaller (< 3 µm) domains of amorphous OM, but absent from the larger OM domains. (B) Richardson 13221, calc. 1.51 %Ro. The pores are more rounded than in immature Woodford OM, but the size range of the larger pores (80 and 140 nm) is similar to that in the immature amorphous OM. The larger OM domains are non-porous. (C) Richardson 13221, calc. 1.51 %Ro. Only smaller domains of amorphous OM are porous, larger domains are commonly featureless and appear homogeneous. (D) Mather Ranch 5 McM#5, 3.1% VRo. Large organic pores in addition to irregular shaped 100s nm scale pores and residual organic coatings on pores that are otherwise defined by adjacent mineral grains.

are undoubtedly primary depositional features in structured organic matter such as the algal colonies (Figs. 3A and 5A), but the primary nature of pores within amorphous organic matter is less clear given the uncertain origin of amorphous sedimentary organic matter. For example, SEM analysis of modern transparent exopolymer particles (Turk et al., 2010; Verdugo et al., 2004) suggests that amorphous sedimentary OM interpreted to be of 'marine snow' origin (Macquaker et al., 2010) is likely to feature abundant primary organic pores, although these may not survive early diagenesis and compaction. However, 'primary' pores may also be the product of low-temperature, early diagenetic microbial reworking of deposited OM (Pacton et al., 2011). In any case, the term 'primary' is useful here to distinguish pores in immature organic matter from 'secondary' pores in thermally mature organic matter which may be linked to thermogenic alteration and hydrocarbon expulsion.

The presence of pores within thermally immature organic matter has long been known. However, there has not been a systematic SEM-based evaluation of such porosity, including its fate during burial and thermal maturation. Our results show that primary pores are common within certain classes of OM in thermally immature mudrocks. We hypothesise that the absence of pores

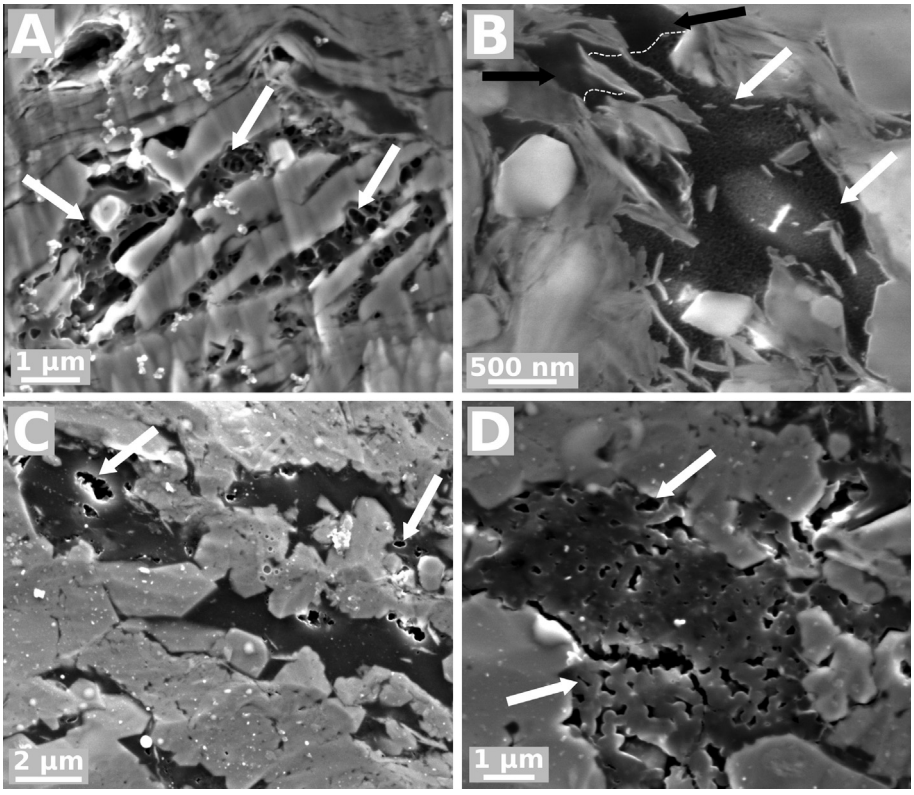

Fig. 9. Organic pores evident in Ar ion milled, solvent extracted Woodford shale samples of oil maturity. The absence of OM-hosted pores prior to solvent extraction (Figs. 6 and 7) indicates that these are filled with bitumen, which is indistinguishable from kerogen using electron optical techniques. (A) EF 3412, calc. 0.51 %Ro. Abundant OM-hosted pores where OM is located between elongate quartz grains. Pores are not evident in the OM domains encapsulated by clays. (B) Holt 3690.8, calc. 1.09 %Ro. Abundant nanopores in otherwise amorphous organic matter evident only after solvent extraction. Note the transition from non-porous to porous OM marked by the dashed line. (C) Chitwood Harris 14911.9, calc. 0.95 %Ro. nm to µm size pores in amorphous OM domain. (D) Chitwood Harris 14911.9, calc. 0.95 %Ro. Abundant large, potentially interconnected pores in a large OM particle interpreted as a degraded Tasmanites.

in all OM types within oil-mature samples reflects modification of OM during thermal maturation of the kerogen, and that the primary OM-hosted porosity identified here influences subsequent pore development into the gas window.

4.1. Mechanisms of primary pore loss with thermal maturation

The Woodford Shale shows porosity in immature OM that is not apparent in samples from the oil window, but returns with a similar morphology in examples from the gas window. The absence of organic-hosted pores in oil-mature Woodford samples may simply be a product of the marked microscale sample to sample variability in texture, mineralogy as well as OM class and distribution that is commonly evident even in mudrock samples of the same lithofacies and thermal maturity (e.g. Aplin and Macquaker, 2011; Curtis et al., 2012a). This microscale heterogeneity is compounded across the relatively small areas that can be imaged at the required resolution. The dearth of pores within oil-mature OM, however, is consistent across the multiple samples imaged, and with previous studies (Curtis et al., 2012a; Loucks et al., 2012), so that burial or diagenetic transformations leading to a loss of primary pores is a more likely explanation for their absence.

Two mechanisms potentially explain the absence of OM-hosted pores in oil-mature Woodford Shale samples. Firstly, this may be caused by compaction associated with burial and thermal maturation of the sediment (Fishman et al., 2012; Milliken et al., 2014). Increased OM plasticity at greater temperatures may further contribute to the loss of intragranular OM porosity. Another possibility is that the apparent absence of primary pores is due to their filling by bitumen generated by thermal cleaving of kerogen associated with the onset of the oil window. Petroleum generation involves the cleaving of weak non-covalent bonds in kerogen to form a macromolecular bitumen phase. This commences at approximately 50 °C (> 1–2 km depth), followed by cleavage of covalent bonds in bitumen to form liquid oil and natural gas at greater temperatures and depths (Seewald, 2003; Stainforth, 2009). Bitumen is thought to be able to diffuse through the kerogen macromolecular structure (Stainforth and Reinders, 1990; Stainforth, 2009), and it has been argued that at least a portion of the bitumen generated during initial thermal maturation of the kerogen is retained within the kerogen without being expelled (Stainforth and Reinders, 1990; Pepper and Corvi, 1995; Vandenbroucke and Largeau, 2007; Stainforth, 2009). Retention of bitumen by kerogen is indicated by: (a) bitumen extract yields which correlate with TOC, (b) higher carbon-normalised extract yields at maturities corresponding to the oil window, (c) carbon-normalised extract yields that are not substantially reduced after removal of the inorganic matrix by acid treatment, and (d) the observation that, except for the most fractured of source rocks, the volume of bitumen in cracks and intergranular pores can only account for a small fraction of total rock bitumen content (Stainforth and Reinders, 1990; Pepper and Corvi, 1995; Stainforth, 2009). In addition, it has been shown that a fraction of bitumen, known as bitumen II, is retained by oil-mature kerogen following whole-rock solvent extraction and can only be extracted after removal of the mineral matrix with strong acids (Wilhelms et al., 1991). There is thus a body of evidence indicating retention of bitumen by kerogen.

Recent work showing an increase in bulk micropore volume after solvent extraction of high TOC mudrocks (Valenza et al., 2013) and coal (Furmann et al., 2013), in particular for

oil-mature samples, supports a hypothesis in which bitumen retention results in filling of OM-hosted pores, followed by their evacuation as bitumen is expelled at higher thermal maturities. This would also explain the re-emergence of pores similar to the primary pores observed in thermally immature OM (e.g. Fig. 8A). Bitumen infilling would effectively mask the presence of OM-hosted pores given that there is insufficient compositional contrast to distinguish between kerogen and bitumen using backscatter electron imaging, the primary imaging approach used. However, bitumen and lighter hydrocarbons are defined on the basis of their solubility in organic solvents (Hunt, 1996), offering a means by which to test this hypothesis. SEM imaging of Woodford Shale samples subject to a 72 h Soxhlet extraction reveals a marked increase in organic pore abundance in solvent extracted, oil-mature subsamples relative to untreated subsamples (Fig. 9). Thus, although not readily evident using standard electron imaging techniques, organic pores are abundant in oil-mature Woodford samples. Increased pore abundance following bitumen removal is particularly apparent in samples from the Chitwood-Harris and Holt cores, where pores are evident in most OM classes, excluding woody OM but including classes such as Tasmanites which did not exhibit primary pores in thermally immature samples. The less class-specific distribution of OM-hosted pores in solvent-extracted oil-mature samples then raises the question of whether the newly visible pores are mainly primary in origin, mainly secondary products of thermal maturation or, as seems most likely, a mixture of the two. Our findings contrast with those of Milliken et al. (2013), where changes OM porosity after solvent extraction and re-imaging of late oil-mature (ca. 1 %Ro), high TOC Marcellus Shale samples of Devonian age were not observed, although an increased abundance of mineral-hosted pores was observed. Their results may be attributed to: (a) absence of OM-hosted pores, (b) pore loss mainly by compaction, (c) solvent contact times insufficient to mobilise pore-filling bitumen, or (d) pore filling by organic phase that is not readily solvent-extractable (Behar and Vandenbroucke, 1988). The opening of mineral-hosted pores observed by Milliken et al. (2013) after solvent extraction, however, suggests mobilisation of bitumen and does not support scenarios (c) and (d). It seems that in this example generated bitumen was not retained by the kerogen, migrating into the relatively larger mineral-hosted pores instead.

Unless accompanied by migration of hydrocarbons along a connected organic pore network from intervals of greater thermal maturity, filling of primary pores by bitumen requires volumetric expansion. The conversion of kerogen to bitumen, and subsequently to liquid hydrocarbons, is associated with a volumetric expansion of ca. 20% (Hunt, 1996) as relatively higher density kerogen of 1.25–1.18 g/cm^3 (Okiongbo et al., 2005) is converted to bitumen (ca. 1 g/cm^3) and liquid hydrocarbons (ca. 0.95–0.76 g/cm^3; Stasiuk and Snowdon, 1997). Overpressure attributed to this conversion is considered one of the main drivers of primary migration (Hunt, 1996). The infilling of organic pores may thus be a purely local process brought on by volumetric expansion during bitumen and liquid hydrocarbon formation, without requiring further compaction coincident with the oil window. The limited generative capacity of woody OM may then account for the persistence of primary pores in oil-mature discrete woody organic particles, as observed in the Jurassic Kimmeridge Clay Fm (Fishman et al., 2012).

4.2. Does primary porosity influence secondary porosity development?

Not only do our results suggest that primary porosity is widespread in thermally immature OM, it is also likely that primary OM-hosted porosity influences the distribution and morphology of at least some of the pores found in late oil-mature to gas-mature samples, particularly in structured organic matter. We observed pores between sub-μm size oblate/spherical OM bodies and slit-like pores associated with colonial algal material in thermally immature samples from both the Woodford Shale (Fig. 5A) and the Stuart Range Formation (Fig. 3D). Although these features are absent in both the oil-mature Woodford samples imaged here and those studied by Curtis et al. (2012a), the pores associated with the oblate OM bodies are present in the gas-mature Woodford samples from the Richardson core (Fig. 8A), implying a degree of inheritance or expulsion of a hydrocarbon phase that filled and thus masked these pores in oil-mature samples. While we did not observe slit-like pores in the small number of gas-mature Woodford samples imaged for this study, Loucks et al. (2012) observed OM with aligned, slit-like pores in gas-mature samples of the Mississippian Barnett Shale.

Similarities in shape, distribution and size of primary pores within amorphous OM and the pores typical of many gas-mature mudrocks, particularly in the smaller porous OM domains, may be further indication of a primary pore influence on secondary pore formation (compare Figs. 5A–D and 8A–C). The equant shape of the pores present in immature amorphous OM is similar to those described in the literature for gas-mature samples, although these are somewhat smaller and more angular in the immature Woodford samples (Wyche core) compared to the rounded pores in gas-mature Woodford samples (Richardson core). It has been suggested that organic pores in gas-mature samples may develop within bitumen rather than in primary kerogen (Bernard et al., 2012; Loucks et al., 2012; Milliken et al., 2013; Schieber, 2013), on the basis of the round morphology of the pores, which is considered to be indicative of ex-solvation of a gaseous phase within bitumen. If correct, this would signify that the development of secondary porosity was largely independent of primary OM structure, as bitumen is a quasi-solid derivative of kerogen that has no structural relation to the precursor kerogen (Vandenbroucke and Largeau, 2007). However, the bitumen or pyrobitumen nature of the porous, gas-mature OM domains remains unclear, largely because established organic petrology techniques used to identify bitumen involve light microscopy that cannot resolve the μm-scale OM domains in question. In any case, our observation of round pores of similar size in thermally immature kerogen demonstrates that these pores can form via different pathways (Fig. 2C and D and Fig. 3B) and are not necessarily restricted to bitumen. Furthermore, Milliken et al. (2013) note that complex, mineral associated and discrete sponge-like pores in thermally mature OM tend to cluster together, rather than being uniformly distributed. Not only is pore clustering apparent in the gas-mature Richardson core samples studied here, this is also typical of pores within the amorphous-type OM prevalent within the thermally immature Monterey, Demerara Rise and Woodford samples, so that pore clustering is not an attribute unique to gas bubble pores formed in bitumen.

Thus, although further work is required to clarify the extent of primary porosity and kerogen structure influence on the development of secondary pores in both structured and amorphous OM, the similarities between primary and secondary pores, together with our identification of pore filling bitumen, argue for such an influence. What mechanisms can account for such a ‘structural inheritance’? Where the loss of primary porosity during the early oil window is primarily due to filling of pores by bitumen, continued heating resulting in removal of bitumen by expulsion or secondary cracking could lead to re-emergence of pre-existing pores. Even where loss of primary pores is related mainly to compaction, compacted pores may be retained as points of weakness within the kerogen structure, these perhaps being more prone to thermal cracking and loss of generated hydrocarbons. Certainly, inheritance of porosity from original OM properties helps explain

the occurrence of porous OM adjacent to non-porous OM observed in several previous studies (Curtis et al., 2012a; Loucks et al., 2012), where thermal maturation cannot be the only controlling factor because the adjacent OM domains have experienced the same burial history. Rather this is more likely due to inherent differences in the OM such as: (a) different starting/initial porosity, required for pore re-emergence, limiting porosity development in one OM domain but not the other, or (b) compositional differences of OM so that one generates pores or pore-filling bitumen more readily than the other (i.e. different maceral types such as liptinite vs intertinite). However, the presence of pores in Tasmanites in solvent extracted, oil-mature Woodford Shale samples demonstrates that not all OM-hosted pores observed in gas-mature and overmature samples have a primary pore precursor or influence. In any case, pore development at extreme thermal maturities is unlikely to be strongly influenced by inheritance from primary pore structure, as illustrated by the oversize pores within overmature Woodford samples (Fig. 8D). If there is a primary pore influence on pore distribution at this thermal maturity, then pore growth and coalescence associated with maturation and hydrocarbon generation has masked this influence.

4.3. Potential implications for hydrocarbon storage and migration

The organic porosity trends identified here have implications for hydrocarbon retention and migration. Conflicting views exist on the physical processes controlling migration of petroleum through organic-rich rocks, with some models arguing that primary migration occurs via Darcy flow through the inorganic pore network (Pepper and Corvi, 1995) and others assuming that petroleum migrates by 'activated diffusion' through a continuous network of kerogen (Stainforth and Reinders, 1990; Stainforth, 2009). What is common to these models is the assumption that generated petroleum or bitumen is retained by and remains associated with the kerogen until it is ultimately expelled. In both cases, these models would predict that as the early oil window is reached and HCs are generated and retained within the kerogen, sub-μm pores would be masked as they are filled with the retained HCs, until that point where their expulsion occurs. Our results demonstrate masking of primary OM-hosted porosity in the earliest oil window, through infilling with a generated bitumen phase that is indistinguishable from the primary kerogen using electron optical techniques, as well as early generation of secondary pores which remain filled with the generated product. Infilling of pores by a mobile generated hydrocarbon implies that primary pores remain open in regard to HC migration throughout the oil window, and that secondary pores contribute to this network in the mid to late oil window. OM-hosted pores may thus represent an alternative physical mechanism for the passage of HCs through kerogen which has otherwise been attributed to 'activated diffusion' of HC molecules through the kerogen macromolecular structure (Stainforth, 2009). In this case organic pores would play a greater role in primary HC migration and hydrocarbon storage, across a wider range of thermal maturities, than is currently appreciated – well developed organic pore networks contributing to permeability and storage capacity are otherwise assumed to be a feature characteristic of gas-mature systems.

5. Conclusions

Our results show that primary OM-hosted pores are common in both structured and amorphous organic matter in thermally immature (pre-oil window) mudrocks, demonstrating that these pores are not purely a product of thermal maturation. However, not all types of organic matter host primary pores. Their abundance, size and distribution appear to be a function of OM type, with structured OM being most consistent, whereas amorphous OM shows the greatest variability.

A thermal maturity gradient from the Devonian Woodford Shale shows that primary OM-hosted porosity is not evident in electron microscope images at thermal maturities equivalent to the early oil window (%Ro > 0.5), but that secondary pores emerge at thermal maturities with %Ro > 1.51. We propose two mechanisms to explain the loss of primary pores with onset of the oil window: (1) compaction facilitated by deeper burial and thermal plasticity and (2) masking of pores by bitumen retained by and redistributed within the kerogen structure. A marked increase in the abundance of organic-hosted pores after solvent extraction of oil-mature samples supports the latter mechanism.

Similarities with primary pore size, shape and distribution suggest that secondary OM-hosted pore development at higher thermal maturities is influenced by primary organic porosity, either because compacted pores are retained as preferred points of secondary pore formation or because of expulsion of pore-filling bitumen leading to re-emergence of primary pores. Given the heterogeneous distribution of primary OM-hosted pores, a primary porosity influence on secondary porosity helps explain the occurrence or porous OM adjacent to non-porous OM in highly thermally mature samples. Our findings suggest that the organic pore trends with thermal maturity interpreted in some studies may reflect the inability of the electron imaging techniques utilised to discriminate bitumen filled primary pores in samples within the oil window. Treating samples to remove bitumen prior to imaging can be used to identify these pores. Finally, given that bitumen filled OM-hosted pores are likely open in regards to hydrocarbon migration, the importance of organic pore networks for primary migration in the oil window may be significant.

Acknowledgements

We thank the Australian Research Council for financial support (DP110103367 and LP120200086 to MJK) and staff at Adelaide Microscopy (University of Adelaide) for guidance on sample preparation and SEM BSE analysis. Roger Slatt (University of Oklahoma) and Brian Cardott (Oklahoma Geological Survey) generously provided some of the Woodford samples. We thank Kitty Milliken and an anonymous reviewer for comments that helped improve the manuscript. This research also used samples and data provided by the Ocean Drilling Program (ODP). ODP is sponsored by the U.S. National Science Foundation (NSF) and participating countries under management of Joint Oceanographic Institutions (JOI), Inc.

Associate Editor—**Andy Bishop**

References

Aplin, A.C., Macquaker, J.H.S., 2011. Mudstone diversity: origin and implications for source, seal, and reservoir properties in petroleum systems. American Association of Petroleum Geologists Bulletin 95, 2031–2059.

Bahadur, J., Radlinski, A.P., Melnichenko, Y.B., Mastalerz, M., Schimmelmann, A., 2015. Small-angle and ultrasmall-angle neutron scattering (SANS/USANS) study of New Albany Shale: a treatise on microporosity. Energy & Fuels 29, 567–576.

Behar, F., Vandenbroucke, M., 1988. Characterization and quantification of saturates trapped inside kerogen: implications for pyrolysate composition. Organic Geochemistry 13, 927–938.

Bernard, S., Wirth, R., Schreiber, A., Schulz, H.-M., Horsfield, B., 2012. Formation of nanoporous pyrobitumen residues during maturation of the Barnett Shale (Fort Worth Basin). International Journal of Coal Geology 103, 3–11.

Bralower, T.J., Lorente, M.A., 2003. Paleogeography and stratigraphy of the La Luna formation and related Cretaceous anoxic depositional systems. Palaios 18, 301–304.

Comer, J.B., 1991. Stratigraphic Analysis of the Upper Devonian Woodford Formation, Permian Basin, West Texas and Southeastern New Mexico (No. 201). Bureau of Economic Geology, Austin.

Curtis, M.E., Cardott, B.J., Sondergeld, C.H., Rai, C.S., 2012a. Development of organic porosity in the Woodford Shale with increasing thermal maturity. International Journal of Coal Geology 103, 26–31.
Curtis, M.E., Sondergeld, C.H., Ambrose, R.J., Rai, C.S., 2012b. Microstructural investigation of gas shales in two and three dimensions using nanometer-scale resolution imaging. American Association of Petroleum Geologists Bulletin 96, 665–677.
Fishman, N.S., Hackley, P.C., Lowers, H.A., Hill, R.J., Egenhoff, S.O., Eberl, D.D., Blum, A.E., 2012. The nature of porosity in organic-rich mudstones of the Upper Jurassic Kimmeridge Clay Formation, North Sea, offshore United Kingdom. International Journal of Coal Geology 103, 32–50.
Furmann, A., Mastalerz, M., Brassell, S.C., Schimmelmann, A., Picardal, F., 2013. Extractability of biomarkers from high- and low-vitrinite coals and its effect on the porosity of coal. International Journal of Coal Geology 107, 141–151.
Graham, S.A., Williams, L.A., 1985. Tectonic, depositional, and diagenetic history of Monterey Formation (Miocene), central San Joaquin Basin, California. American Association of Petroleum Geologists Bulletin 69, 385–411.
Hunt, J.M., 1996. Petroleum Geochemistry and Geology, second ed. Freeman, W. H.
Isaacs, C.M., 2001. Depositional framework of the Monterey Formation, California. In: Isaacs, C.M., Rullkötter, J. (Eds.), The Monterey Formation – From Rocks to Molecules. Publisher, New York, pp. 31–59.
Jarvie, D.M., Claxton, B.L., Henk, F., Breyer, J.T., 2001. Oil and Shale Gas from the Barnett Shale, Ft. Worth Basin, Texas. Talk presented at the AAPG National Convention, June 3–6, 2001, Denver, CO, American Association of Petroleum Geologists Bulletin, p. A100.
Kennedy, M.J., Löhr, S.C., Fraser, S.A., Baruch, E.T., 2014. Direct evidence for organic carbon preservation as clay-organic nanocomposites in a Devonian black shale; from deposition to diagenesis. Earth and Planetary Science Letters 388, 59–70.
Kirkland, D.W., Denison, R.E., Summers, D.M., Gormly, J.R., 1992. Geology and organic geochemistry of the Woodford Shale in the Criner Hills and western Arbuckle Mountains, Oklahoma. In: Johnson, K.S., Cardott, B.J. (Eds.), Source Rocks in the Southern Mid-Continent: 1990 Symposium. Oklahoma Geological Survey Circular, pp. 38–69.
Löhr, S.C., Kennedy, M.J., 2014. Organomineral nanocomposite carbon burial during Oceanic Anoxic Event 2. Biogeosciences 11, 4971–4983.
Löhr, S.C., Kennedy, M.J., 2015. Micro-trace fossils reveal pervasive reworking of Pliocene sapropels by low-oxygen-adapted benthic meiofauna. Nature Communications. http://dx.doi.org/10.1038/ncomms7589.
Loucks, R.G., Reed, R.M., 2014. Scanning-electron-microscope petrographic evidence for distinguishing organic-matter pores associated with depositional organic matter versus migrated organic matter in mudrocks. Gulf Coast Association of Geological Societies Journal 3, 51–60.
Loucks, R.G., Reed, R.M., Ruppel, S.C., Jarvie, D.M., 2009. Morphology, genesis, and distribution of nanometer-scale pores in siliceous mudstones of the Mississippian Barnett Shale. Journal of Sedimentary Research 79, 848–861.
Loucks, R.G., Reed, R.M., Ruppel, S.C., Hammes, U., 2012. Spectrum of pore types and networks in mudrocks and a descriptive classification for matrix-related mudrock pores. American Association of Petroleum Geologists Bulletin 96, 1071–1098.
Macquaker, J.H.S., Keller, M.A., Davies, S.J., 2010. Algal blooms and "marine snow": mechanisms that enhance preservation of organic carbon in ancient fine-grained sediments. Journal of Sedimentary Research 80, 934–942.
Mastalerz, M., He, L., Melnichenko, Y.B., Rupp, J.A., 2012. Porosity of coal and shale: insights from gas adsorption and SANS/USANS techniques. Energy & Fuels 26, 5109–5120.
Mastalerz, M., Schimmelmann, A., Drobniak, A., Chen, Y., 2013. Porosity of Devonian and Mississippian New Albany Shale across a maturation gradient: insights from organic petrology, gas adsorption, and mercury intrusion. American Association of Petroleum Geologists Bulletin 97, 1621–1643.
Menpes, S.A., 2012. Unconventional hydrocarbon potential of the Arckaringa Basin, South Australia. In: Ambrose, G.J., Scott, J. (Eds.). Talk presented at the Central Australian Basins Symposium III, pp. 1–7.
Meyers, P.A., Bernasconi, S.M., Forster, A., 2006. Origins and accumulation of organic matter in expanded Albian to Santonian black shale sequences on the Demerara Rise, South American margin. Organic Geochemistry 37, 1816–1830.
Miceli Romero, A., Philp, R.P., 2012. Organic geochemistry of the Woodford Shale, southeastern Oklahoma: how variable can shales be? American Association of Petroleum Geologists Bulletin 96, 493–517.
Milliken, K.L., Rudnicki, M., Awwiller, D.N., Zhang, T., 2013. Organic matter-hosted pore system, Marcellus Formation (Devonian), Pennsylvania. American Association of Petroleum Geologists Bulletin 97, 177–200.
Milliken, K.L., Ko, L.T., Pommer, M., Marsaglia, K.M., 2014. SEM Petrography of Eastern Mediterranean sapropels: analogue data for assessing organic matter in oil and gas shales. Journal of Sedimentary Research 84, 961–974.
Nederbragt, A.J., Thurow, J., Pearce, R., 2007. Sediment composition and cyclicity in the mid-Cretaceous at Demerara Rise, ODP Leg 207. In: Mosher, D.C., Erbacher, J., Malone, M.J., Garrison, R.E. (Eds.), Proceedings of the Ocean Drilling Program, Scientific Results, 207. Ocean Drilling Program, College Station TX, pp. 1–31.
Okiongbo, K.S., Aplin, Andrew C., Larter, S.R., 2005. Changes in type II kerogen density as a function of maturity: evidence from the Kimmeridge Clay Formation. Energy & Fuels 29, 567–576.
Pacton, M., Gorin, G.E., Vasconcelos, C., 2011. Amorphous organic matter – experimental data on formation and the role of microbes. Review of Palaeobotany and Palynology 166, 253–267.
Pepper, A.S., Corvi, P.J., 1995. Simple kinetic models of petroleum formation. Part III: modelling an open system. Marine and Petroleum Geology 12, 417–452.
Schieber, J., 2013. SEM Observations on ion-milled samples of Devonian Black Shales from Indiana and New York: the petrographic context of multiple pore types. In: Camp, W., Diaz, E., Wawak, B. (Eds.), Electron Microscopy of Shale Hydrocarbon Reservoirs: American Association of Petroleum Geologists Memoir 102. pp. 153–171.
Seewald, J.S., 2003. Organic-inorganic interactions in petroleum-producing sedimentary basins. Nature 426, 327–333.
Senftle, J.T., 1989. Influence of kerogen isolation methods on petrographic and bulk chemical composition of Woodford Shale round robin sample: Report of the TSOP Research Committee. Presented at the The Society for Organic Petrology (TSOP) 6th Annual Meeting, pp. 1–1.
Sherrod, L., Dunn, G., Peterson, G., Kolberg, R., 2002. Inorganic carbon analysis by modified pressure-calcimeter method. Soil Science Society of America Journal 66, 299–305.
Shipboard Scientific Party, 2004. Leg 207 Summary. In: Erbacher, J., Mosher, D.C., Malone, M.J. (Eds.), Proceedings of the Ocean Drilling Program, Initial Reports. Ocean Drilling Program, College Station, TX.
Slatt, R.M., Buckner, N., Abousleiman, Y., Sierra, R., Philp, P., Miceli Romero, A., Portas, R., O'Brien, N.R., Tran, M., Davis, R., Wawrzyniec, T., 2011. Outcrop/behind outcrop (quarry), multiscale characterization of the Woodford Gas Shale, Oklahoma. In: Breyer, J.T. (Ed.), Shale Reservoirs – Giant Resources for the 21st Century. American Association of Petroleum Geologists Memoir 97, 1–21.
Stainforth, J.G., 2009. Practical kinetic modeling of petroleum generation and expulsion. Marine and Petroleum Geology 26, 552–572.
Stainforth, J.G., Reinders, J.E.A., 1990. Primary migration of hydrocarbons by diffusion through organic-matter networks, and its effect on oil and gas generation. Organic Geochemistry 16, 61–74.
Stasiuk, L.D., Snowdon, L.R., 1997. Fluorescence micro-spectrometry of synthetic and natural hydrocarbon fluid inclusions: crude oil chemistry, density and application to petroleum migration. Applied Geochemistry 12, 229–241.
Suárez-Ruiz, I., Flores, D., Filho, J.M., Hackley, P.C., 2012. Review and update of the applications of organic petrology: part 1, geological applications. International Journal of Coal Geology 99, 54–112.
Takashima, R., Nishi, H., Huber, B.T., Leckie, R.M., 2006. Greenhouse world and the Mesozoic ocean. Oceanography 19, 82–92.
Taylor, G.H., Teichmüller, M., Davis, A., Diessel, C.F.K., Littke, R., Robert, P., 1998. Organic Petrology. Gebrüder Borntraeger, Berlin.
Telnova, O.P., 2012. Morphology and ultrastructure of Devonian prasinophycean algae (Chlorophyta). Paleontological Journal 46, 543–548.
Turk, V., Hagstrom, A., Kovac, N., Faganeli, J., 2010. Composition and function of mucilage macroaggregates in the northern Adriatic. Aquatic Microbial Ecology 61, 279–289.
Valenza, J.J., Drenzek, N., Marques, F., Pagels, M., Mastalerz, M., 2013. Geochemical controls on shale microstructure. Geology 41, 611–614.
Vandenbroucke, M., Largeau, C., 2007. Kerogen origin, evolution and structure. Organic Geochemistry 38, 719–833.
Verdugo, P., Alldredge, A., Azam, F., Kirchman, D., Passow, U., Santschi, P., 2004. The oceanic gel phase: a bridge in the DOM-POM continuum. Marine Chemistry 92, 67–85.
Wilhelms, A., Larter, S.R., Leythaeuser, D., 1991. Influence of bitumen-2 on Rock-Eval pyrolysis. Organic Geochemistry 17, 351–354.